Supplementary Information (SI) for Soft Matter.

(Supporting Information) Revealing Intrinsic Electric Double Layer Viscoelasticity in Ionic Liquid Solutions via Quartz Crystal Microbalance

Atsushi Matsumoto[a,*], Ryota Yoshizawa[b], Riccardo Funari[c], Osamu Urakawa[b], Tadashi Inoue[b], and Amy Q. Shen[d,*]

[a]Department of Applied Chemistry and Biotechnology, Graduate School of Engineering, University of Fukui
[b]Department of Macromolecular Science, Graduate School of Science, The University of Osaka
[c]Institute of Mechanical Intelligence, Scuola Superiore Sant'Anna, Via G. Moruzzi, 1, Pisa 56124, Italy
[d]Micro/Bio/Nanofluidics Unit, Okinawa Institute of Science and Technology Graduate University
[*]Corresponding authors: AM: atsushi5@u-fukui.ac.jp; AS: amy.shen@oist.jp

S1 Wave propagation model and its limitations

The solute concentration c_s range where the wave propagation model described in Section 2.6.2 of the main manuscript is applicable for estimating the complex modulus of the electric double layer (EDL) in IL solutions.

Our wave propagation model [1] assumes that the effects of the change in the density ρ_B and shear viscosity η_B of the bulk solution on the resonant frequency and the energy dissipation of a quartz can be captured by using the Kanazawa-Gordon model [2]. Their model accounts for the oscillation of a quartz crystal immersed in a Newtonian fluid, and predicts the change of the resonant frequency $f_B(c_s)$ with respect to that in air as:

$$f_B(c_s) = -f_0^{\frac{3}{2}} \sqrt{\frac{\eta_B \rho_B}{\pi \rho_q G_q}}, \tag{S1}$$

where f_0 is the fundamental frequency, $\rho_q = 2.648$ g cm^{-3} the density, and $G_q = 2.947 \times 10^{11}$ g cm^{-1} s^{-2} the storage shear modulus of the AT-cut quartz crystal.

In order to check the validity of the Kanazawa-Gordon model, given by Eq. S1, we measured the resonant frequency of a quartz immersed in the mixture of non-ionic ethylene glycol (EG) and water at $f_0 = 10$ MHz. Fig. S1 compares the measured frequency $|\Delta f_{exp}|$ shift with that predicted by Eq. S1. Here, $\Delta f_{exp} = f_{exp}(c_s) - f_{exp}(0)$ represents the change of the resonant frequency in EG solutions with respect to those in pure water at $c_s = 0$ M, and its absolute value of $|\Delta f_{exp}|$ is plotted in Fig. S1 to highlight the change

in the resonant frequency. We found that the value of $|\Delta f_{\rm exp}|$ agreed with the predicted value of $|\Delta f_{\rm B}|$ for $c_{\rm s} < 8$ M, beyond which our experimental data deviated significantly from the predicted curve by the Kanazawa-Gordon model. We hypothesize that the observed discrepancy between the experimental data and the theoretical prediction could be explained by considering that the oscillation of the quartz became insensitive to the change in the density and viscosity of the bulk solution at high $c_{\rm s}$. Indeed, the amplitude of the quartz oscillation reduced almost to the level of the baseline at high $c_{\rm s}$, as shown in Fig. 5 of the main manuscript.

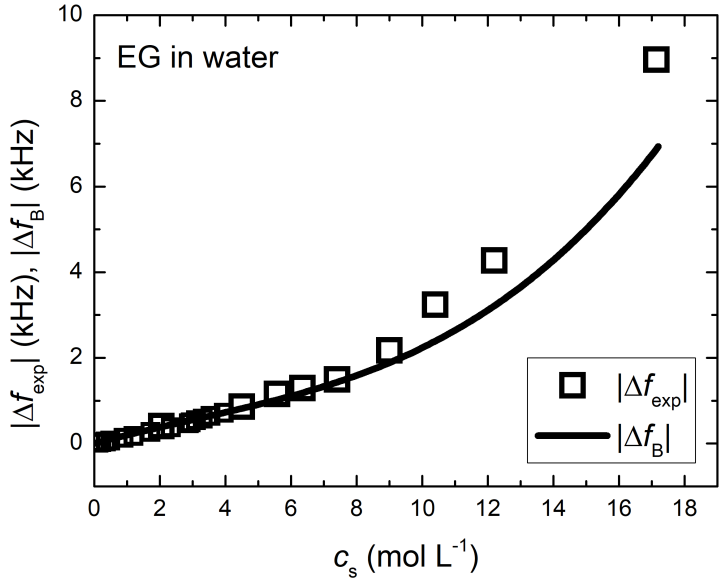

Figure S1: Comparison of the resonant frequency shift between the experimental data $|\Delta f_{\rm exp}|$ (black squares) and the theoretical prediction $|\Delta f_{\rm B}|$ (solid line), given by Eq. S1, for the mixture of ethylene glycol and water. The values of $|\Delta f_{\rm exp}|$ and $|\Delta f_{\rm B}|$ at 25°C are plotted as a function of the EG concentration $c_{\rm s}$.

Based on the observation above, we propose that the value of $\sqrt{\rho_{\rm B}\eta_{\rm B}}$ may provide a reliable criterion for the measurable $c_{\rm s}$ range where the Kanazawa-Gordon model is valid. Fig. S2 shows the dependence of $\sqrt{\rho_{\rm B}\eta_{\rm B}}$ on $c_{\rm s}$ for aqueous solutions of EG. Since a deviation of $|\Delta f_{\rm exp}|$ from $|\Delta f_{\rm B}|$ started at $c_{\rm s} \sim 8$ M, the corresponding level of $\sqrt{\rho_{\rm B}\eta_{\rm B}}$ is shown as the dashed line in Fig. S2. We now compare this guideline with the dependence of $\sqrt{\rho_{\rm B}\eta_{\rm B}}$ on $c_{\rm s}$ for Bmim-TFSI, Bmim-TfO, and Bmim-BF_4 solutions in DMF. The value of $\sqrt{\rho_{\rm B}\eta_{\rm B}}$ for the IL solution increased monotonically with increasing $c_{\rm s}$. More importantly, the measured $\sqrt{\rho_{\rm B}\eta_{\rm B}}$ intersected with the dashed guideline at $c_{\rm s} \sim 1.9$ M for Bmim-TFSI, $c_{\rm s} \sim 2$ M for Bmim-TfO, and $c_{\rm s} \sim 2.5$ M for Bmim-BF_4 solutions. As a result, we restrict our QCM experiments to solutions at IL concentrations around the crossover concentration for each IL mixture to avoid the potential breakdown of the Kanazawa-Gordon model, given by Eq. S1.

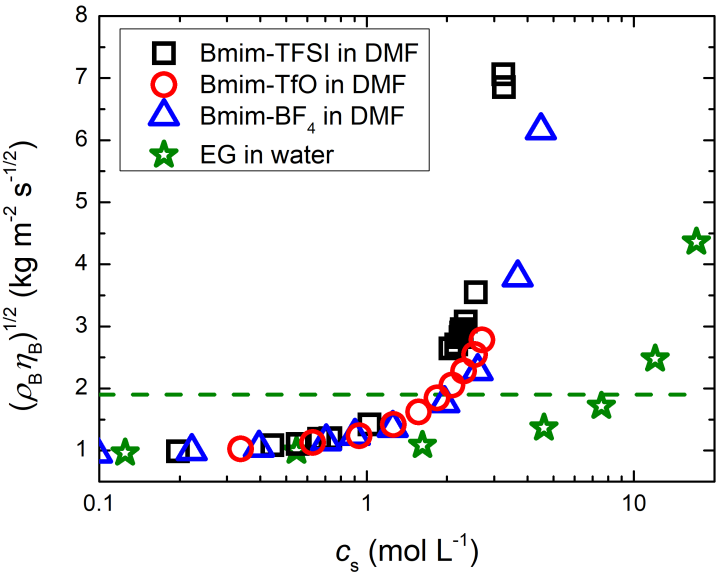

Figure S2: The dependence of the square root of the product of the density ρ_B and shear viscosity η_B on the solute concentration c_s for Bmim-TFSI (black squares), Bmim-TfO (red circles), Bmim-BF_4 (blue triangles) solutions in DMF and aqueous solutions of EG (green stars). The dashed line represents the value of $\sqrt{\rho_B \eta_B}$ beyond which the Kanazawa-Gordon model, given by Eq. S1, becomes inapplicable for EG solutions.

S2 Linear Viscoelasticity of Bulk Solutions

To justify the assumption that the bulk solution behaves as a Newtonian fluid at high frequencies QCM employed, we measured the complex modulus $G^* = G' + iG''$ for the mixture of Bmim-TFSI and DMF at $c_s = 2.53$ M by using a strain-controlled shear rheometer (ARES-G2, TA Instruments). Fig. S3 shows the dependence of the complex modulus G^* at 25°C on the angular frequency ω, obtained by applying the time-temperature superposition (TTS) principle to the G^* data measured in the ω range of $0.1 \leq \omega \leq 100$ rad s^{-1} at various temperatures. Specifically, we shifted the G^* data horizontally using the shift factor a_T so that the obtained composite curve of the loss modulus G'' at low ω follows the scaling of $G'' = \eta_B \omega$ predicted by the zero-shear viscosity η_B of the mixture at 25°C. In Fig. S3, the storage modulus G' was much smaller than the loss modulus G'' at low frequencies, and the difference in magnitude between G' and G'' became small as the frequency increased. Finally, G' became larger than G'' at high frequencies. More importantly, we found that the value of G'' followed the predicted scaling of $G'' \propto \omega$ for $\omega < 10^{10}$ Hz, while that of G' was scaled as $G' \propto \omega^2$ in the same frequency range. The obtained G^* spectra were typical for glass-forming molecular solvents, and similar ω dependence of G^* was observed for pure ionic liquids [3, 4] At 10 MHz where our QCM employed, G'' was much greater than G' and lay on the slope of $G'' = \eta_B \omega$. These results indicate that the bulk solution at $c_s = 2.53$ M behaves as a Newtonian fluid at 10 MHz.

We now discuss if the assumption is still valid at lower c_s we investigated. We anticipate that the analysis with the TTS principle, discussed above, no longer holds at lower c_s because the solution mixture may form crystalline structures at lower c_s due to the crystallinity of pure DMF around −60°C [5]. When the solution mixture crystal-

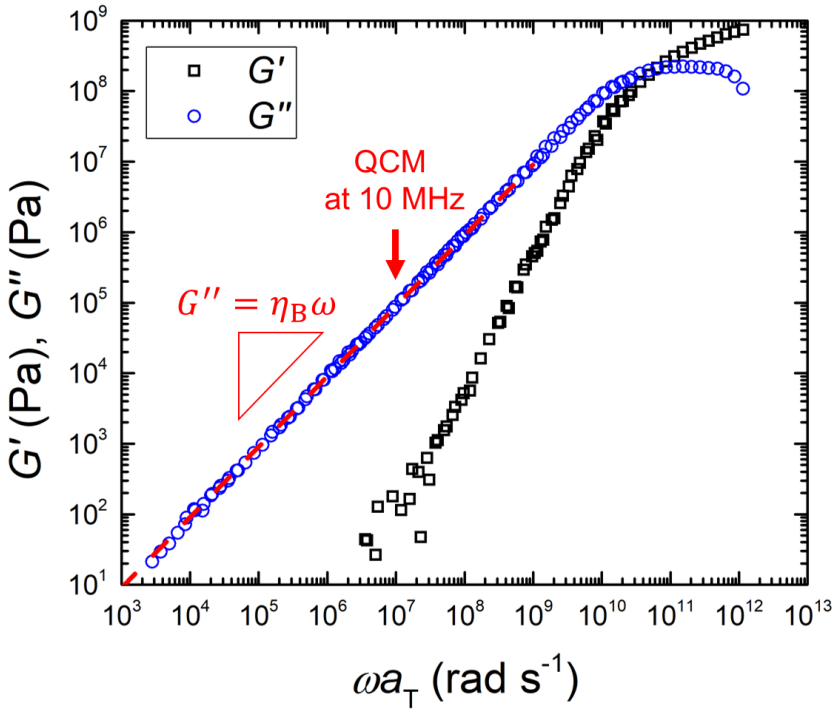

Figure S3: The composite curve of the complex modulus $G^* = G' + iG''$ for the mixture of Bmim-TFSI and DMF at $c_s = 2.53$ M. The reference temperature is set at 25°C. The red dashed line represents the predicted curve of G'' at low c_s, given as $G'' = \eta_B \omega$, where η_B denotes the zero-shear viscosity at 25°C of the solution mixture. The red arrow indicates the G'' data at 10 MHz where openQCM Q-1 employs.

lizes, the TTS principle no longer holds since the structure changes before and after the melting point. In this case, it is challenging to obtain the G^* data at frequencies around 10^7 Hz by using the strain-controlled shear rheometer. Nevertheless, it is still possible to imagine how the G^* spectra changes as the ionic liquid concentration decreases. Here, we assume that the shape of G^* spectra is independent of c_s, based on the fact that the frequency dependence of G^* for glass-forming molecular solvents is very similar to each other [3, 4, 6]. In other words, we assume that the G^* spectra for a given c_s can be obtained by shifting horizontally the G^* spectra shown in Fig. S3. The degree of shift can be determined from the variation of η_B with c_s. In Fig. 3 of the main manuscript, we observed that the value of η_B decreases with decreasing c_s. This result indicates that the red dashed line in Fig. S3 would shift to the right side of the graph as c_s decreases. As a result, the value of G'' at 10 MHz becomes smaller while lying on the slope of $G'' = \eta_B \omega$, suggesting that the bulk solution retains a Newtonian response at lower c_s. The same argument can potentially hold for ionic liquids with different anions because McKenna and co-workers [3, 4] reported that the dependence of G^* on ω was independent of the chemical structure of ionic liquid cations and anions. Although we cannot provide direct evidence, our experimental results support our assumption that our bulk solutions behave as a Newtonian fluid in the c_s range investigated.

S3 Supporting figure

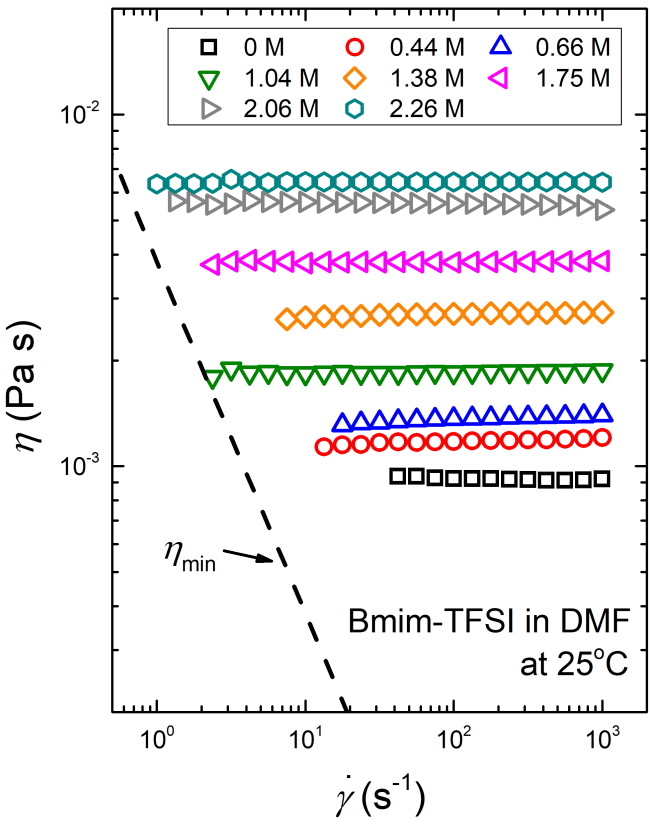

Figure S4: Shear viscosity curves for the mixture of Bmim-TFSI and DMF at various concentrations of Bmim-TFSI. In the plot, the shear viscosity η at 25°C is plotted as a function of the shear rate $\dot{\gamma}$. The dashed black line represents the minimum level of η that can be measured accurately using a strain-controlled rheometer (ARES-G2, TA Instruments) with a stainless steel cone and plate geometry having 50 mm in diameter and 1° in cone angle. The value of η_{min} is calculated as $\eta_{\mathrm{min}} = \frac{3T_{\mathrm{min,ss}}}{2\pi R^3 \dot{\gamma}}$ [7], where $T_{\mathrm{min,ss}}$ and R are the minimum measurable torque in steady state and the cone radius, respectively. Note that for ARES-G2, $T_{\mathrm{min,ss}}$ is specified as $T_{\mathrm{min,ss}} = 0.1$ μN by the manufacturer, but we chose $T_{\mathrm{min,ss}} = 1$ μN m as a more conservative value.

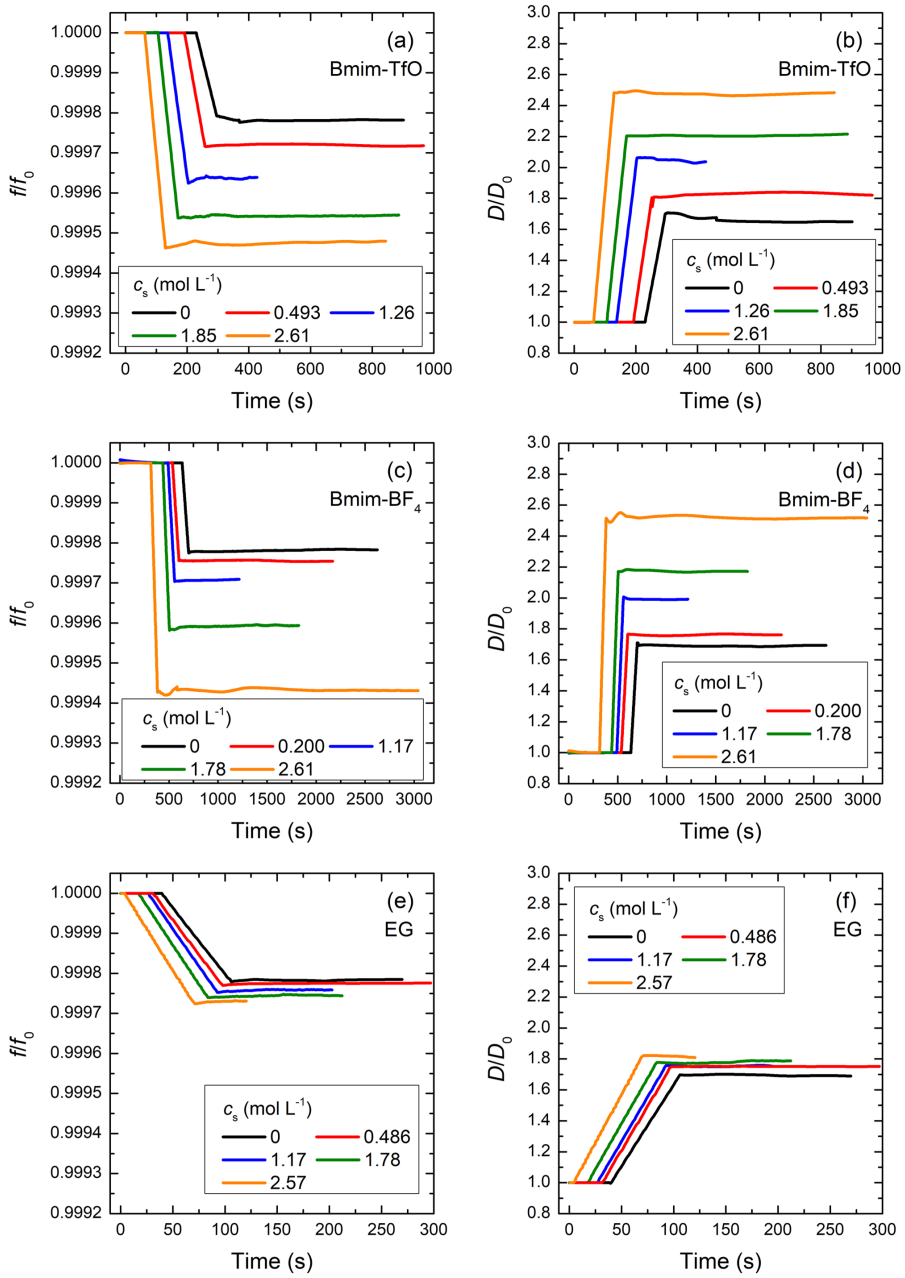

Figure S5: Representative QCM sensorgrams at 25°C for (a & b) Bmim-TfO, (c & d) Bmim-BF_4, and (e & f) EG solutions in DMF at various solute concentrations c_s. In the plot, the values of the resonant frequency f and the energy dissipation D of the quartz crystal in the solution are normalized by the fundamental frequency f_0 and dissipation D_0 of the oscillating quartz in air. The curves are horizontally shifted for clarity purposes.

References

[1] R. Funari, A. Matsumoto, J. R. de Bruyn, A. Q. Shen, Rheology of the electric double layer in electrolyte solutions, Anal. Chem. 92 (12) (2020) 8244–8253.

[2] K. Keiji Kanazawa, J. G. Gordon, The oscillation frequency of a quartz resonator in contact with liquid, Anal. Chim. Acta 175 (1985) 99–105.

[3] N. Shamim, G. B. McKenna, Glass dynamics and anomalous aging in a family of ionic liquids above the glass transition temperature, J. Phys. Chem. B 114 (48) (2010) 15742–15752.

[4] R. Tao, S. L. Simon, Rheology of imidazolium-based ionic liquids with aromatic functionality, J. Phys. Chem. B 119 (35) (2015) 11953–11959.

[5] W. M. Haynes, CRC handbook of chemistry and physics, CRC press, 2014.

[6] S. A. Hutcheson, G. B. McKenna, The measurement of mechanical properties of glycerol, m-toluidine, and sucrose benzoate under consideration of corrected rheometer compliance: An in-depth study and review, J. Chem. Phys. 129 (7) (2008) 074502.

[7] R. H. Ewoldt, M. T. Johnston, L. M. Caretta, Experimental challenges of shear rheology: how to avoid bad data, in: Complex Fluids in Biological Systems, Springer, 2015.